GMR
The Original

GREEN SYNTHESIS OF CuO NANOPARTICLES LOADED WITH POLYMERIC NANOSCAFFOLDS FROM *Sargassum muticum* EXTRACT: STRUCTURAL INSIGHTS INTO ANTICANCER ACTIVITY ON HT-29 AND MCF-7 CELLS

Akshayaa Paramasivan[1], Chakradhar Arepalli[2], Sattanathan Govindharajan[3]*

[1]Saveetha Medical College & Hospital (SMCH), Saveetha Institute of Medical and Technical Sciences (SIMATS), Thandalam, Chennai, Tamil Nadu 602105, India. akshivan1965@gmail.com
[2]Department of Nephrology, Saveetha Medical College and Hospital, Saveetha Institute of Medical And Technical Sciences (SIMATS), Thandalam, Chennai-602105, Tamil Nadu, India. Email: arepalli.chakri@gmail.com
[3]Department of Pathology, Saveetha Medical College and Hospital, Saveetha Institute of Medical And Technical Sciences (SIMATS), Thandalam, Chennai-602105, Tamil Nadu, India. Email: sattanathanphd@gmail.com
*Corresponding Author: sattanathanphd@gmail.com (S.G.)

ABSTRACT

The present study outlines an eco-friendly ultrasonic method to produce CuO nanoparticles from Sargassum muticum extract and embed them into starch–PVA nanofibers. UV-Vis analysis showed a 270 nm absorption peak, while FTIR confirmed functional groups involved in nanoparticle formation and stabilization, while X-ray diffraction (XRD) confirmed a monoclinic crystalline structure (JCPDS 05-0661). Scanning electron microscopy (SEM) imaging demonstrated uniform nanoparticle dispersion within the porous, fibrous nanoscaffold matrix, and Thermogravimetric analysis (TGA) indicated thermal stability up to 243°C. Dynamic light scattering (DLS) revealed a particle size of 92.1 nm with moderate colloidal stability (zeta potential: −12.62 mV). The anticancer activity of the extract, CuO nanoparticles, and starch/PVA/CuO-loaded scaffolds was tested on HT-29 and MCF-7 cells. The composite scaffolds showed the moderate cytotoxic response, with IC_{50} values of 12 µg/mL and 20 µg/mL, outperforming both the nanoparticles and the crude extract. These results highlight the scaffold's enhanced therapeutic potential, likely due to improved nanoparticle delivery and bioavailability. The findings position starch/PVA/CuO-NPs nanoscaffolds as a promising platform for targeted cancer therapy, warranting further mechanistic and *in vivo* investigations.

KEYWORDS: *Sargassum muticum*, Biogenic CuONPs, Starch/PVA/CuONPs nanoscaffolds, Anticancer activity.

1. INTRODUCTION

Nanotechnology has revolutionized the field of biomedical sciences by enabling the development of multifunctional nanomaterials with tailored properties for therapeutic applications [1]. Among these, metal oxide nanoparticles, such as copper oxide nanoparticles (CuO NPs), have garnered significant attention due to their unique physicochemical features, including high surface area, stability, catalytic activity, and inherent biological functionalities [2]. These properties make CuO NPs promising candidates for anticancer therapies, antimicrobial agents, and drug delivery systems [3]. However, conventional chemical synthesis methods of CuO NPs often involve toxic reagents and harsh conditions, raising concerns about environmental safety and biocompatibility [2]. In this context, green synthesis using natural extracts has emerged as an eco-friendly, sustainable alternative that not only reduces the environmental footprint but also imparts additional biological activity through phytochemical capping agents [4].

Marine macroalgae, widely recognized for their rich reservoir of bioactive compounds such as polyphenols, flavonoids, terpenoids, and polysaccharides, represent an underexplored source for the biogenic synthesis of nanoparticles [5]. Among these, *Sargassum muticum*, a brown marine macroalgae commonly found in intertidal zones, exhibits a potent array of antioxidants and secondary metabolites with diverse pharmacological properties including anti-inflammatory, antimicrobial, and anticancer effects [6]. Harnessing the phytoconstituents of *S. muticum* as reducing and stabilizing agents in the synthesis of CuO NPs not only facilitates particle formation under mild conditions but also potentially enhances the therapeutic efficacy of the nanoparticles through synergistic bioactivity [7].

Ultrasonic-assisted extraction techniques have been increasingly adopted to enhance the yield and efficacy of bioactive compound retrieval from natural sources [8]. The cavitation effect generated by ultrasound waves disrupts plant cell walls and promotes efficient mass transfer, enabling the release of phytochemicals in higher concentrations compared to conventional methods [9]. Utilizing ultrasound-assisted extraction of *S. muticum* extract for the biogenic synthesis of CuO NPs thus offers a dual advantage: improved extraction efficiency of

active biomolecules and facilitation of nanoparticle formation with desirable characteristics such as uniform size distribution and surface functionalization [10, 11].

For effective biomedical applications, particularly in cancer therapy, nanoparticle delivery systems must possess biocompatibility, controlled release profiles, and the ability to interact favorably with biological tissues [12]. Electrospun nanofibrous scaffolds fabricated from biopolymers provide an excellent platform to address these needs [13]. Electrospinning is a versatile and facile technique capable of producing continuous fibers with nanoscale diameters, high porosity, and interconnected pore structures, closely mimicking the extracellular matrix (ECM) [14]. Such scaffolds support cell adhesion, proliferation, and controlled release of incorporated therapeutic agents [15]. Blending natural polysaccharides such as starch with synthetic polymers like polyvinyl alcohol (PVA) combines the advantages of biodegradability, mechanical strength, and processability, yielding scaffolds with desirable physicochemical and biological properties [16].

Incorporation of biogenically synthesized CuO NPs into starch/PVA electrospun scaffolds can potentially create a multifunctional nanocomposite with enhanced anticancer efficacy [17]. The CuO NPs act as active agents that can induce reactive oxygen species (ROS) generation within cancer cells, leading to oxidative stress-mediated apoptosis, while the polymeric matrix ensures sustained delivery and biocompatibility [18]. Additionally, the phytochemical coating derived from *S. muticum* may further potentiate anticancer effects and reduce systemic toxicity [19]. Such integrative nanoscaffolds open new avenues for localized cancer treatment, minimizing side effects commonly associated with systemic chemotherapy [20].

Although previous studies have explored the biosynthesis of CuO NPs using various terrestrial plant extracts and their incorporation into polymeric matrices, the combination of ultrasonic-assisted biogenic synthesis from marine macroalgae and electrospinning of starch/PVA nanofibers remains largely unexplored [21]. Moreover, the comprehensive physicochemical characterization of these novel nanoscaffolds and their evaluation against human cancer cell lines such as colon adenocarcinoma (HT-29) and breast cancer (MCF-7) is crucial for validating their therapeutic potential [22]. Parameters such as particle size, surface charge, crystallinity, thermal stability, fiber morphology, and nanoparticle dispersion within the scaffold matrix directly influence biological interactions and anticancer efficacy [23].

Therefore, the present study focuses on the green synthesis of CuO NPs using ultrasonic-assisted aqueous extract of *S. muticum*, followed by their incorporation into starch/PVA electrospun nanofibers [24]. The study aims to thoroughly characterize the physicochemical properties of the synthesized nanoparticles and the resulting nanoscaffolds using spectroscopic, microscopic, and thermal analytical techniques [25]. Furthermore, it evaluates the anticancer potential of these nanocomposites through *in vitro* cytotoxicity assays on HT-29 and MCF-7 cell lines [26]. This approach not only emphasizes sustainable nanoparticle synthesis leveraging marine resources but also offers innovative nanofibrous biomaterials that could advance cancer therapeutics [27].

2. MATERIALS AND METHODS

2.1. Collection and preparation of marine macroalgae

Specimens of *S. muticum* were manually collected from intertidal zones along the coastal region near Rameswaram. The collected *Sargassum muticum* was taxonomically identified and authenticated by Dr V. Veeragurunathan, CSIR-CSMCRI-Marine Algal Research Station, Mandapam Camp 623519, Tamil Nadu, India. A voucher specimen was prepared and deposited at the Herbarium of the CSIR-CSMCRI-Marine Algal Research Station, under the accession number: SI–2025–RMM–016. This authentication ensures botanical accuracy and standardization of the study material. Immediately after collection, samples were stored in chilled containers to maintain freshness during transport to the laboratory. Upon receipt, the algal biomass was rinsed thoroughly with running tap water to remove sand, debris, and epiphytic organisms. This cleaning was followed by multiple washes with distilled water to achieve purity. The cleaned algae were then cut into small segments and dried naturally in a shaded, ventilated environment at room temperature for about two weeks. After complete drying, the samples were ground into a fine powder using a mechanical grinder, and the powder was stored in airtight containers at ambient conditions until further use.

2.2. Phytochemical extraction by ultrasonic treatment

For the extraction of phytochemicals, 2g of excellently ground *S. muticum* were mixed with 50 mL of Milli-Q water and processed in a LABQUEST ultrasonic bath (Borosil; Serial No. 941032329018) at 60 °C for 45 minutes. Ultrasonic cavitation improved the release of active constituents. The extract was then passed through Whatman No.1 filter paper to obtain a clean aqueous filtrate. The extract was temporarily stored at 4°C and subsequently freeze-dried using a lyophilizer for long-term preservation and downstream applications [28, 29].

2.3. Green synthesis of CuO NPs

The biosynthesis of CuO NPs was carried out by mixing 50 mL of 0.1 M $CuSO_4 \cdot 5H_2O$ solution with 10 mL of *S. muticum* extract, prepared by dissolving 10 mg of lyophilized powder in 10 mL Milli-Q water, maintaining a volume ratio of 5:1. The combined solution was stirred continuously at 650 rpm and heated at 60°C for 2 hours. A visible shift from blue to a bluish-green tint indicated the successful reduction of copper ions and nanoparticle formation. The resulting mixture was centrifuged, and the collected pellet was rinsed three times with double-distilled water to eliminate remaining impurities and organic residues. The purified nanoparticles were freeze-

dried for 48 hours and stored in a moisture-free container for further characterization and incorporation into scaffolds [30].

2.4. Electrospinning of starch/PVA nanofibers containing CuO NPs

For nanocomposite fiber preparation, a 15% (w/w) PVA solution was first prepared in Milli-Q water with continuous stirring until completely dissolved. To this, 100 mg each of starch and CuO nanoparticles were incorporated, and the mixture was kept at 50 °C with vigorous stirring for 2.5 hours to achieve uniform dispersion. The resulting blend was transferred to a syringe equipped with a stainless-steel needle (0.84 mm internal diameter) and mounted on the HOLMARC HO-NFES-040 electrospinning unit. Optimal electrospinning conditions included an applied voltage of 11.5 kV, a 12.3 cm tip-to-collector distance, and a feed rate of 0.4 mL/h. The electrospinning process was carried out at room temperature for 6 to 8 hours, and the resulting nanofiber mats were collected and stored in a desiccator for future use and characterization [31-33].

2.5. Physicochemical characterization of nanoparticles and electrospun mats

2.5.1. UV-Vis spectroscopic analysis

Optical properties of the *S. muticum* extract and the synthesized CuO NPs were analyzed using a VIS SPEC V-730 spectrophotometer, scanning wavelengths from 200 to 800 nm. Deionized water served as the blank. The presence of characteristic surface plasmon resonance (SPR) peaks indicated successful nanoparticle formation [34].

2.5.2. Fourier-transform infrared (FTIR) spectroscopy

FTIR analysis was carried out on a PerkinElmer Spectrum Two system using ATR mode. Spectra were collected between 4000 and 400 cm^{-1} at a resolution of 4 cm^{-1}, with 64 scans for each sample. The identified bands corresponded to hydroxyl, phenolic, carbonyl, and metal–oxygen functional groups [35].

2.5.3. X-ray diffraction (XRD) analysis

X-ray diffraction was performed using a Bruker D8 Advance system equipped with CuKα radiation (λ = 1.5406 Å) and operated at 40 kV and 40 mA. Diffraction patterns were recorded across a 2θ range of 5° to 90°, using a step interval of 0.029649°. The diffraction peaks were compared with standard JCPDS data to confirm CuO phase purity [36].

2.5.4. Scanning Electron Microscope (SEM) imaging

Surface features and nanoparticle distribution were analyzed using a JEOL JSM-IT800 NANO scanning electron microscope. Before imaging, the samples were coated with a thin layer of gold to improve surface conductivity and obtain clear micrographs. SEM images were analyzed to measure fiber diameters, nanoparticle distribution, and surface structure [37].

2.5.5. Thermogravimetric Analysis (TGA)

Thermogravimetric analysis was performed using a PerkinElmer TGA 8000 to evaluate the stability of the nanofiber composites. Roughly 5 mg of each sample was heated from ambient temperature to 550 °C at a controlled rate of 15 °C/min under a nitrogen atmosphere. TGA curves provided insight into moisture loss, polymer degradation, and residual mass [38].

2.5.6. Particle size and zeta potential

The hydrodynamic size distribution and surface charge of CuO NPs were measured using a Malvern Zetasizer Ultra. Zeta potential values were used to evaluate the colloidal stability, where higher absolute values suggested strong electrostatic repulsion and stable dispersions [39].

All experimental datasets are publicly accessible in the Mendeley Data repository, DOI: 10.17632/jrs2y2hp7v.2.

2.6. *In vitro* anticancer activity

2.6.1. Cell procurement and culture

HT-29 colon cancer cells and MCF-7 breast cancer cells were sourced from the National Centre for Cell Science (NCCS), Pune, India. Both cell lines were maintained according to NCCS guidelines in Minimum Essential Medium (MEM) supplemented with 10% FBS and incubated at 37 °C in a 5% CO_2-humidified environment [26].

2.6.2. MTT assay for cell viability

HT-29 and MCF-7 cell lines, procured from the National Centre for Cell Science (NCCS), Pune, were used as authenticated models for evaluating anticancer effects. Cells were plated at a density of 5×10^5 cells per well in 96-well plates and allowed to settle overnight. Treatments with *S. muticum* extract, CuO nanoparticles, and starch/PVA/CuO nanoscaffolds were applied at concentrations of 6.25, 12.5, 25, 50, and 100 µg/mL, each in triplicate, and cultures were incubated for 24 hours at 37 °C in a 5% CO_2 atmosphere. After treatment, 20 µL of MTT reagent was added to each well and left for 4 hours to allow for formazan formation. The resulting crystals were dissolved in 200 µL of DMSO, and absorbance was measured at 570 nm. Experiments were repeated thrice independently for reproducibility. Mean absorbance values and standard deviations were calculated for data analysis [40].

2.7. Statistical analysis

Data analysis was carried out using SPSS 25.0 and GraphPad Prism 9.0. Results from triplicate assays are presented as mean ± standard deviation. Group differences were evaluated using one-way ANOVA with Tukey's

or Dunnett's post-hoc comparisons where applicable, considering $p < 0.05$ as statistically significant. Normality was examined using the Shapiro–Wilk test, and datasets that failed this criterion were log-transformed prior to further analysis. Pearson's correlation was used to explore associations between variables, and all findings were interpreted within a 95% confidence interval [41].

3. RESULTS

3.1. UV–visible spectroscopy

UV–Visible spectra for both the *S. muticum* extract and the synthesized CuO nanoparticles were obtained using a JASCO V-730 spectrophotometer across 200–800 nm with a 1 nm interval (Fig. 1). The extract showed characteristic absorption linked to its bioactive compounds, whereas the CuO nanoparticles displayed a clear plasmon-related peak at about 270 nm, confirming their successful formation. The absorbance value at this peak was measured at 0.4776, confirming successful synthesis of CuO NPs. Instrument parameters, including a slit width of 1.0 nm, scan speed of 1000 nm/min, and automatic filter adjustments, contributed to accurate spectral capture. These findings highlight the unique optical signatures of CuO NPs compared to the original marine extract, verifying their nanoscale generation.

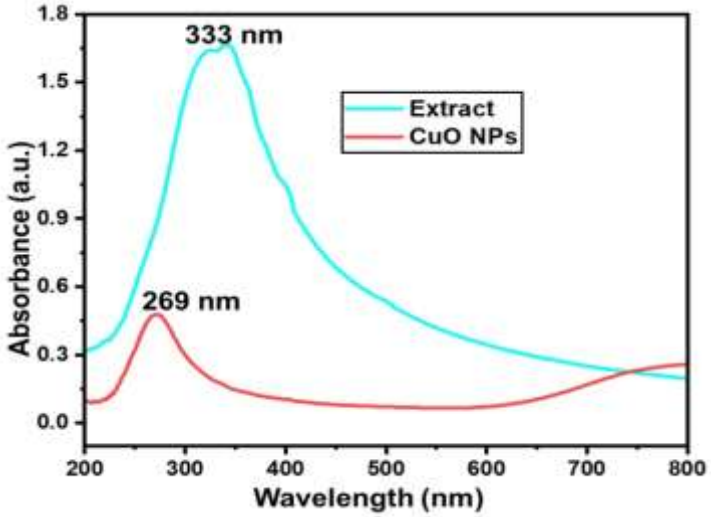

Fig. 1. UV–Visible absorption spectra comparing the *S. muticum* extract with the synthesized CuO nanoparticles.

3.2. FTIR spectroscopy

FTIR spectra of the CuO NPs and starch/PVA nanoscaffolds were collected in ATR mode with a PerkinElmer Spectrum Two spectrometer, scanning from 4000 to 400 cm^{-1} at 4 cm^{-1} resolution (Fig. 2). The CuO NPs showed broad O–H stretching vibrations centered at 3277 cm^{-1}, accompanied by absorption bands near 2700 and 2500 cm^{-1}, which suggest C–H stretching and possible carbonyl functional groups. The starch/PVA scaffold exhibited pronounced C=O stretching at 1500 cm^{-1} and a notable peak around 840 cm^{-1} attributed to glycosidic bond vibrations. Bands below 1000 cm^{-1}, particularly near 600 cm^{-1}, corresponded to Cu–O bonding, affirming the successful incorporation of copper oxide within the polymeric network. Overall, these spectral signatures confirm both the preservation of key functional groups and the effective embedding of CuO NPs into the nanofiber matrix.

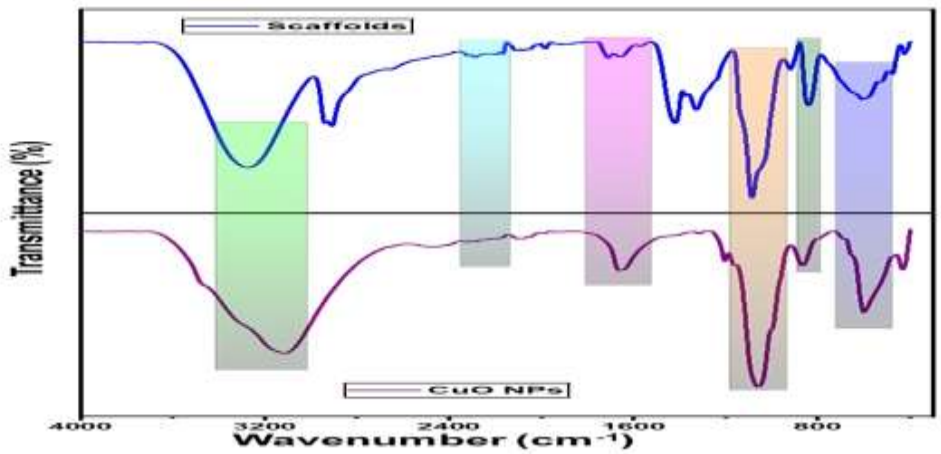

Fig. 2. FTIR profiles of the synthesized CuO nanoparticles and the corresponding starch/PVA nanoscaffolds containing CuO nanoparticles.

3.3. XRD analysis

XRD patterns were obtained using a Bruker D8 Advance diffractometer with CuKα radiation (λ = 1.5406 Å), scanning 2θ angles from 5° to 90°. The CuO NPs exhibited prominent diffraction peaks at 32.7° (110), 35.3° (002), 38.3° (111), and 48.1° (202), characteristic of a monoclinic crystalline structure and matching the JCPDS card no. 05-0661. The starch/PVA electrospun scaffold displayed semicrystalline diffraction peaks at 19.3°, 21.4°, and 23.5°, with additional reflections near 26.5° and 29.5° (Fig. 3) attributable to the influence of the incorporated CuO NPs. The interplanar d-spacing was calculated as 2.73 Å for CuO NPs and 4.60 Å for the scaffolds, corroborating the crystalline integrity of the nanoparticles and their homogeneous dispersion throughout the polymer matrix.

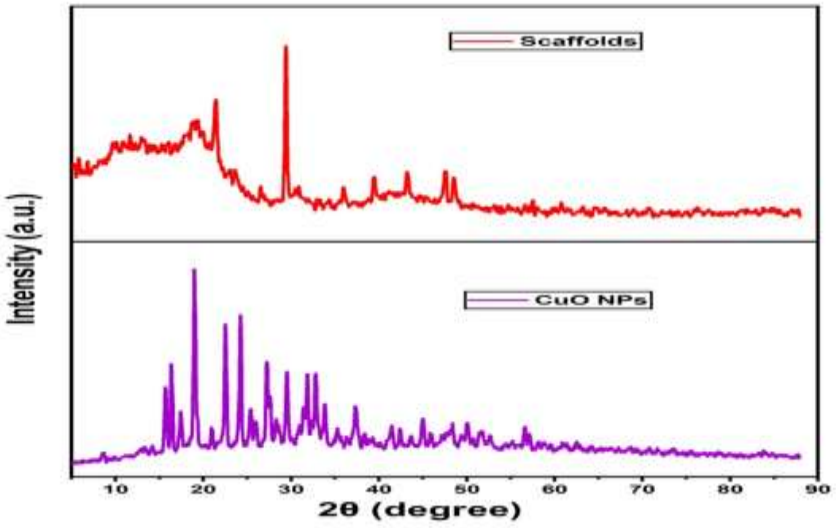

Fig. 3. X-ray diffraction patterns of the prepared CuO nanoparticles and the nanoscaffolds incorporating CuO nanoparticles.

3.4. SEM analysis

SEM images acquired with the JEOL JSM-IT800 NANO microscope revealed morphological differences between pure CuO NPs and the starch/PVA composite nanoscaffolds (Fig. 4). CuO NPs appeared as aggregated clusters displaying spherical to irregular shapes, while the nanofiber scaffold exhibited a porous, fibrous architecture with a relatively smooth surface and minor bead formations. Nanoparticles were uniformly dispersed on the scaffold surface, demonstrating effective loading and integration. The scaffold's porous nature and fibrous morphology suggest its suitability for biomedical applications that require high surface area and mechanical support.

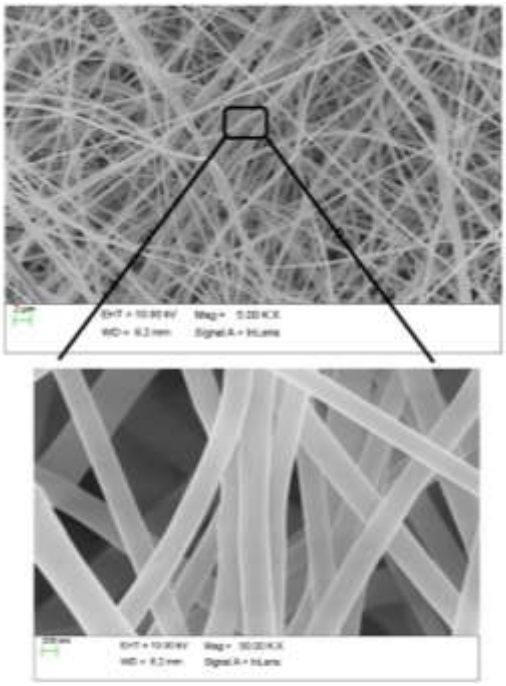

Fig. 4. Scanning electron micrographs showing the morphology of the synthesized CuO nanoparticles and the surface structure of the CuO-infused nanoscaffolds.

3.5. TGA

Thermal stability and decomposition behavior of the nanocomposite scaffolds were investigated using under nitrogen atmosphere from 25°C to 550°C (Fig. 5). The weight loss profile showed three distinct phases: initial moisture evaporation below 150°C, main degradation of polymer components beginning at 243.0°C and peaking at 349.6°C, and a residual mass of approximately 51.9%. The significant mass loss between 200°C and 400°C corresponds primarily to starch and PVA polymer decomposition. The substantial residual mass indicates the presence of thermally stable crosslinked structures or inorganic content such as CuO NPs, confirming that the scaffold maintains structural integrity up to around 243°C.

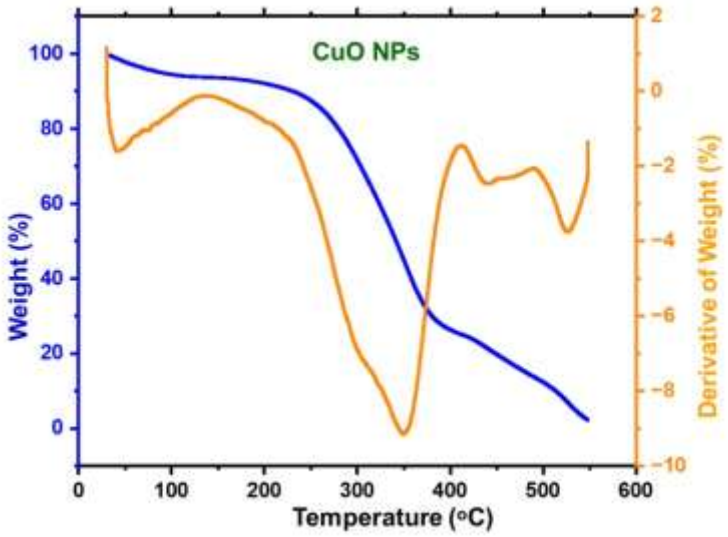

Fig. 5. Thermogravimetric analysis illustrating the degradation profile of the nanoscaffolds containing CuO nanoparticles.

3.6. Zeta potential and particle size analysis

Dynamic light scattering (DLS) measurements determined the hydrodynamic diameter of the biosynthesized CuO NPs to be 92.1 nm with a polydispersity index (PDI) of 0.8444, suggesting a moderately broad size distribution (Fig. 6). The zeta potential analysis revealed a negative surface charge of −12.62 mV, with prominent peaks at −20.85 mV and −8.99 mV (Fig. 7), indicating moderate colloidal stability primarily due to electrostatic repulsion. The system's conductivity was recorded at 0.07909 mS/cm, and a quality factor of 5.109 underscored the reliability of measurements. Collectively, these parameters reflect that the synthesized CuO NPs possess sufficient stability for suspension and incorporation into polymer matrices.

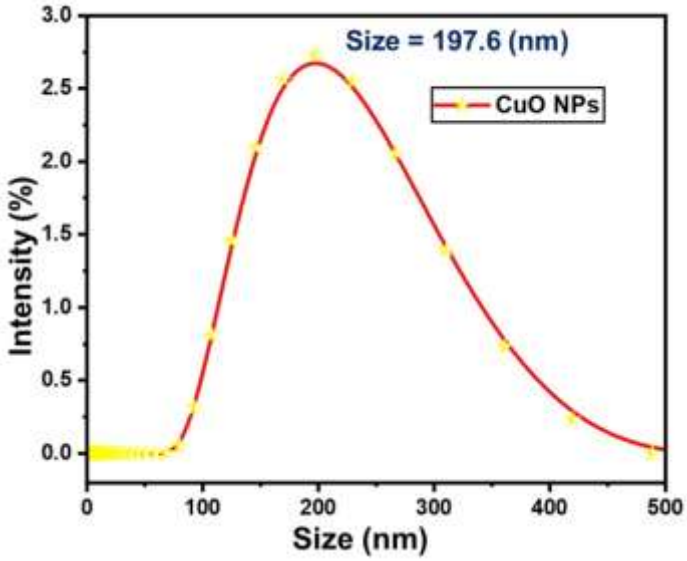

Fig. 6. Dynamic light scattering profile showing the particle size distribution of the synthesized CuO nanoparticles.

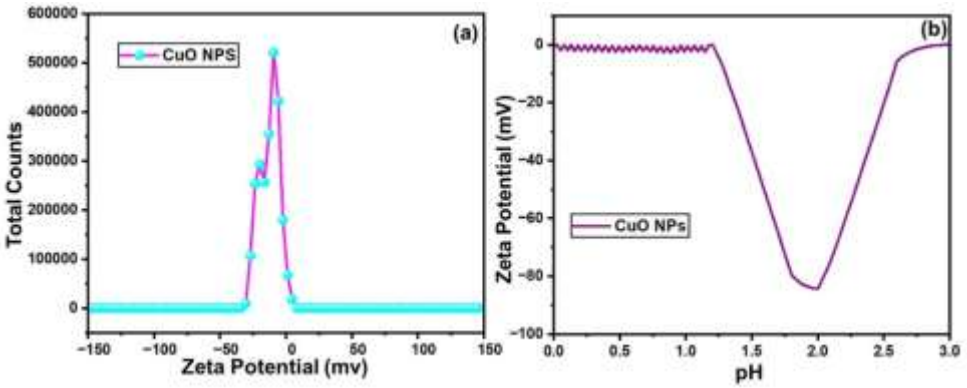

Fig. 7. Zeta potential measurement depicting the surface charge and stability of the synthesized CuO nanoparticles.

3.7. *In vitro* anticancer activity

The anticancer potential of the *S. muticum* extract, CuO nanoparticles, and the starch/PVA/CuO-NP scaffolds was assessed in vitro using the MTT assay on HT-29 colon cancer cells and MCF-7 breast cancer cells (Fig. 8). All treatments produced a concentration-dependent decline in cell viability, though their effectiveness varied across the three formulations. Against the HT-29 cell line, the algal extract exhibited moderate cytotoxicity, reducing cell viability from 100% (control) to 35.25% at the highest tested concentration of 100 µg/mL. The half-maximal inhibitory concentration (IC_{50}) for the algal extract was calculated to be approximately 30 µg/mL, indicating its ability to induce significant cell death at moderate doses. In comparison, CuO NPs displayed stronger anticancer activity, lowering cell viability to 24.83% at 100 µg/mL, with an IC50 value of 18 µg/mL. This suggests that the metallic nanoparticles possess enhanced cytotoxic properties compared to the crude algal extract. However, the most potent effect was observed with the starch/PVA/CuO-NPs nanoscaffolds, which reduced HT-29 cell viability to just 17.88% at 100 µg/mL and exhibited an IC50 of 12 µg/mL. This remarkable efficacy highlights the advantage of the nanoscaffold formulation in improving the delivery or bioavailability of the active components. Similarly, in MCF-7 breast cancer cells, the algal extract reduced cell viability to 49.05% at 100 µg/mL, with an IC50 value of 40 µg/mL. While this indicates a measurable anticancer effect, it was less pronounced than that of the other formulations. CuO NPs demonstrated greater cytotoxicity, decreasing viability to 40.47% at the same concentration, with an IC50 of 28 µg/mL. Once again, the starch/PVA/CuO-NPs nanoscaffolds outperformed both the extract and the standalone nanoparticles, achieving a viability reduction to 27.42% at 100 µg/mL and an IC50 of 20 µg/mL. These findings suggest that the nanoscaffold system enhances the therapeutic potential of CuO NPs, possibly through improved cellular uptake or sustained release mechanisms.

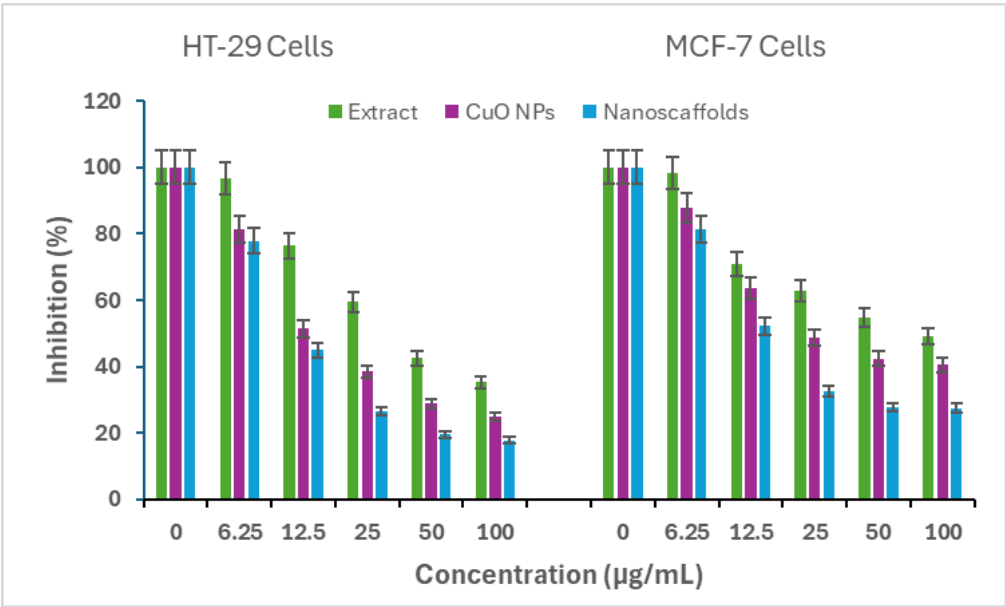

Fig. 8. Comparative anticancer effects of the *S. muticum* extract, CuO nanoparticles, and starch/PVA/CuO-NP nanoscaffolds on cancer cell lines.

The comparative analysis of IC50 values across both cell lines reveals a consistent trend: the starch/PVA/CuO-NPs nanoscaffolds exhibit the highest anticancer activity, followed by CuO NPs, and then the algal extract. This hierarchy suggests that the nanoscaffold formulation not only enhances the efficacy of CuO NPs but also provides a more effective therapeutic approach than the crude extract alone. The improved performance of the nanoscaffolds could be attributed to their structural properties, such as increased surface area, controlled release

kinetics, or enhanced interaction with cancer cells. These results underscore the potential of starch/PVA/CuO-NPs nanoscaffolds as a promising candidate for further development in cancer therapy, warranting additional studies to elucidate their mechanisms of action and evaluate their performance in *in vivo* models.

4. DISCUSSION

The optical characterization of the biosynthesized CuO NPs via UV–Visible spectroscopy revealed a distinctive surface plasmon resonance (SPR) peak at 270 nm, which serves as a critical hallmark confirming nanoparticle formation. The observed SPR peak, absent in the original *S. muticum* extract, clearly differentiates the synthesized nanostructures from the bulk phytochemical components. This characteristic absorption arises from collective electron oscillations on the nanoparticle surface, validating the successful reduction of copper ions to CuO NPs. The precise spectral data obtained under controlled instrumental parameters further substantiates the reproducibility of the biosynthesis process. The shift and intensity of the SPR band indicate nanoscale dimensions and confirm the optical properties intrinsic to CuO, which are essential for subsequent biological applications [42-47].

FTIR spectroscopy provided valuable insights into the chemical interactions and structural integrity of the synthesized nanoparticles and their integration within the starch/PVA nanoscaffolds. The broad O–H stretching vibration observed near 3277 cm^{-1} in CuO NPs suggests the presence of surface hydroxyl groups or adsorbed moisture, which can influence nanoparticle stability and surface reactivity. Peaks associated with C–H and possible carbonyl groups denote residual phytochemical capping agents, implicating bio-organic molecules in the stabilization of the nanoparticles during synthesis. The scaffold's FTIR spectra revealed characteristic bands corresponding to starch and PVA functional groups, with the prominent C=O stretching vibration at 1500 cm^{-1} confirming the polymeric matrix's chemical composition. Notably, the Cu–O bond vibration near 600 cm^{-1} is definitive evidence of CuO NP incorporation within the scaffold, signifying successful physical embedding without disrupting the polymer network. These spectral observations collectively confirm that the nanocomposite preserves essential functional groups, which are likely pivotal for biocompatibility and therapeutic efficacy [48-53].

XRD analysis reinforced the crystalline nature of the synthesized CuO NPs, with diffraction peaks matching the monoclinic phase outlined in standard reference data (JCPDS 05-0661). The retention of crystalline structure post-synthesis is crucial for the nanoparticles' functional properties, including catalytic and biomedical activities. The semicrystalline nature of the starch/PVA scaffold, as indicated by characteristic peaks at 19.3°, 21.4°, and 23.5°, suggests partial crystallinity typical of such biopolymer blends, which can influence mechanical strength and degradation profiles. Importantly, the additional reflections detected near 26.5° and 29.5° in the nanocomposite confirm the homogeneous dispersion of CuO NPs within the polymer matrix, potentially enhancing scaffold functionality through synergistic interactions. The calculated d-spacing values further substantiate the retention of crystallinity and uniform nanoparticle distribution, which are vital for consistent performance in biomedical contexts [54-59].

SEM imaging elucidated the morphological distinctions between the bare CuO NPs and the composite scaffolds. The nanoparticles' aggregated clusters with spherical to irregular shapes align with typical biosynthesis outcomes, where bio-organic molecules often induce agglomeration. The scaffold's porous, fibrous structure with minor bead formations is characteristic of electrospun polymer blends, providing a high surface area that can facilitate cellular interactions and nutrient exchange. The uniform distribution of CuO NPs on the scaffold surface observed in SEM images confirms effective loading, an essential factor for ensuring consistent therapeutic effects. The scaffold morphology, combining porosity with mechanical integrity, suggests suitability for applications such as tissue engineering or drug delivery, where scaffold architecture critically influences biological response [60-67].

TGA highlighted the thermal stability and decomposition behavior of the nanocomposite scaffold. The three-stage weight loss profile is typical for polymeric systems containing inorganic fillers. Initial moisture loss below 150°C reflects surface-adsorbed water, while the major degradation between 243°C and 350°C corresponds to the breakdown of starch and PVA chains. The significant residual mass (~51.9%) after heating indicates the presence of thermally stable components, primarily CuO NPs and possibly crosslinked polymer domains formed during scaffold fabrication. This residual fraction suggests that the nanocomposite can withstand physiological temperatures without significant structural compromise, which is critical for maintaining scaffold integrity during biomedical use. The TGA data collectively demonstrate that the scaffold's thermal resilience is enhanced by nanoparticle incorporation, which may also improve its durability in clinical applications [68-72].

DLS and zeta potential analyses provide a comprehensive understanding of nanoparticle size distribution and colloidal stability—two parameters essential for biomedical applicability. The hydrodynamic diameter of approximately 92 nm situates the nanoparticles within the optimal size range for cellular uptake and enhanced permeability. The relatively high polydispersity index (PDI) indicates a moderate size distribution, common in biosynthesized nanoparticles where natural capping agents influence growth kinetics. The zeta potential value of −12.62 mV reflects a moderate negative surface charge, sufficient to confer electrostatic repulsion that prevents rapid aggregation, thereby maintaining nanoparticle dispersion in suspension. The peaks at −20.85 mV and −8.99 mV likely correspond to different surface environments or capping molecules. Combined with the measured conductivity and quality factor, these findings confirm that the nanoparticles remain stable and well-dispersed,

prerequisites for successful incorporation into polymer scaffolds and for their interaction with biological systems [73-77].

The *in vitro* anticancer efficacy of the algal extract, CuO NPs, and starch/PVA/CuO nanoscaffolds against HT-29 and MCF-7 cell lines revealed a clear trend of increasing cytotoxicity from the crude extract to the nanoparticle form and finally to the nanoscaffold formulation. The enhanced potency observed with CuO NPs compared to the extract underscores the value of nanostructuring, which can improve cellular internalization and reactive oxygen species (ROS) generation, leading to apoptosis induction. The superior anticancer activity of the nanoscaffold likely arises from improved bioavailability and controlled release kinetics afforded by the polymer matrix, which can facilitate sustained delivery of CuO NPs to cancer cells. This enhancement is evident from the lower IC50 values obtained with the scaffold, reflecting more effective cell growth inhibition. The porous and fibrous scaffold morphology, combined with nanoparticle integration, probably facilitates greater interaction with the cell membrane and penetration, which are critical for anticancer activity. These results suggest the nanocomposite system holds significant promise as a therapeutic platform, combining the advantages of natural polymers and metal oxide nanoparticles for targeted cancer treatment [78-80].

Overall, the multidisciplinary characterization—from physicochemical properties to biological activity—demonstrates the potential of CuO NP-loaded starch/PVA scaffolds as effective anticancer agents. The synergy between nanoparticle properties and scaffold architecture enables enhanced stability, controlled release, and superior cytotoxicity, warranting further mechanistic and *in vivo* investigations to fully harness this nanocomposite's therapeutic potential

5. CONCLUSION

This work confirmed that *S. muticum* extract can serve as an efficient green route for producing CuO nanoparticles, which were subsequently integrated into starch/PVA nanoscaffolds. Comprehensive characterization verified the presence of uniformly distributed, crystalline CuO particles with marked optical, structural, and thermal features. The nanoscaffolds exhibited a porous, fibrous architecture ideal for biomedical applications, ensuring stable integration of the nanoparticles. Importantly, the *in vitro* anticancer assessments revealed that the starch/PVA/CuO nanoscaffolds significantly enhanced cytotoxicity against HT-29 and MCF-7 cancer cell lines compared to both the crude algal extract and isolated CuO NPs. This improvement highlights the potential of the nanoscaffold system to improve nanoparticle bioavailability and therapeutic efficacy. Overall, the findings underscore the promise of these biopolymer-based nanocomposites as effective and sustainable candidates for anticancer therapy, paving the way for further in-depth biological studies and potential clinical applications.

Ethics declaration: Not Applicable

Data Availability Statement: The full dataset of physiochemical characterization associated with this work is published in Mendeley Data [Dataset] Bioactive nanostructured platforms: Physicochemical assessment of starch scaffolds hybridized with *Sargassum muticum*-copper oxide nanoparticles (DOI: 10.17632/jrs2y2hp7v.2). Disclosure: The material characterization data and figures (e.g., UV, SEM, FTIR, XRD, TGA, Zeta Potential and particle sizer) presented here were generated from a common dataset and are being reused across multiple related studies on nanomaterials. All biological analyses and conclusions are original to each manuscript.

Conflicts of Interest: The authors declare no conflicts of interest.

REFERENCES

[1] Surendran N, Chandrasekaran G, Raju MV, Chandrasekaran MK, Ahalliya RM, Palanisamy CP, Kanniappan GV, Arcot R, Alharbi NS, Thiruvengadam M. Anti-inflammatory potential of ethanolic extract of Maranta arundinacea L.: Insights from COX-2 modulation and oxidative stress analysis. South African Journal of Botany. 2026; 195: 142-151.

[2] Pei J, Senthilkumar MV, Hessini K, Subramaniyam S, Sivaramakrishnan R, Kanniappan GV, Jayaraman S, Palanisamy CP. Green fabrication of starch/PVA/CuO nanoscaffolds using marine macroalgae extract for enhanced anti-inflammatory activity. Sustainable Chemistry and Pharmacy. 2026; 51: 102397.

[3] Balasubramanian V, Loganathan L, Muthuswamy K, Viswanathan TM, Raju MV, Chandrasekaran MK, Ahalliya RM, Poorasamy J, Palanisamy CP, Dominic S, Kanniappan GV. Anticancer therapeutic efficacy of PEGylated β-galactosidase from Aspergillus terreus in DMBA-induced breast cancer: Toxicological, molecular and histopathological evaluation in Wistar rats. International Journal of Biological Macromolecules. 2026; 360: 151856.

[4] Jayaraman S, Eswaran A, Rajagopal P, Palanisamy CP, Veerakumar P, Veeraraghavan VP, Sirasanagandla SR. Neuroendocrine-associated epigenetic factors in cellular senescence: mechanisms and therapeutic implications. Biogerontology. 2026; 27(2): 64.

[5] Ponnusamy B, Rajagopal P, Palanisamy CP, Veeraraghavan VP, Jayaraman S. Mechanistic Exploration of the anticancer activity of Justicia adhatoda Plant Leaf Ethanolic Extract against Colon Cancer Cells: An in silico and in vitro Approach. Asian Pacific Journal of Cancer Prevention. 2026; 27(3): 1069-1080.

[6] Pei J, Saran VS, Sivaramakrishnan R, Kanniappan GV, Pandurangan V, Jayaraman S, Dhayalan VK, Mironescu M, Mironescu ID, Palanisamy CP. Ultrasonic-assisted, Sargassum ilicifolium (brown marine macroalgae)-mediated biogenic synthesis of CuO nanoparticles incorporated in starch/PVA electrospun nanoscaffolds: In vitro safety and antioxidant efficacy assessment. Bioorganic Chemistry. 2026; 173: 109679.
[7] Raj MAPA, Subramaniyam S, Kanniappan GV, Jayaraman S, Palanisamy CP. Sustainable fabrication of starch/PVA/CuO electrospun nanoscaffolds from Turbinaria ornata (marine macroalgae) extract: Physicochemical characterization and antidiabetic evaluation. Kuwait Journal of Science. 2026; 53(2): 100545.
[8] Pei J, Ganesh NS, Subramaniyam S, Sivaramakrishnan R, Kanniappan GV, Jayaraman S, Palanisamy CP. Sustainable fabrication of starch/PVA/CuO electrospun nanoscaffolds from Padina tetrastromatica (Brown macroalgae) extract: Physicochemical characterization and antidiabetic assessment. Sustainable Chemistry One World. 2026; 9: 100195.
[9] Sakthiraj A, Sivaramakrishnan R, Subramaniyam S, Kanniappan GV, Pandurangan V, Jayaraman S, Dhayalan VK, Mironescu M, Mironescu ID, Palanisamy CP. Starch/PVA electrospun nanoscaffolds loaded with ultrasonic-assisted green-synthesis of CuO nanoparticles from marine macroalgae (Gracilaria corticata) extract: Cytotoxicity and antioxidant analysis. Chemical Physics Impact. 2026; 12: 101018.
[10] Raju M, Chandrasekaran MK, Loganathan L, Ahalliya RM, Mironescu M, Mironescu ID, Palanisamy CP, Kanniappan GV. Lipid remodeling and ferroptosis in phosphatidylcholine-mediated tumor–stroma crosstalk. Frontiers in Molecular Biosciences. 2026; 13: 1742305.
[11] Kunamalla R, Panagal M, Palanisamy CP. Biogenic synthesis and fabrication of starch/PVA/CuO electrospun nanoscaffolds from Sargassum ilicifolium (brown marine macroalgae) extract for anticancer activity on HT-29 and MCF-7 cancer cells. Biocatalysis and Agricultural Biotechnology. 2026; 72: 103923.
[12] Pei J, Govindaraj H, Sivaramakrishnan R, Kanniappan GV, Pandurangan V, Dhayalan VK, Mironescu M, Mironescu ID, Jayaraman S, Palanisamy PC. Sustainable fabrication of biopolymer-based (starch/PVA) nanoscaffolds loaded with green-synthesized CuO nanoparticles from Sargassum wightii (marine macroalgae): Cytocompatibility and antioxidant activity. Biomaterials Advances. 2026; 182: 214660.
[13] Pei J, Perumal NC, Meng P, Long Q, Palanisamy CP. Extracellular vesicle-based biosensors for Alzheimer's disease: A new frontier in precision diagnostics. Ageing Research Reviews. 2026; 113: 102904.
[14] Shree P, Sivaramakrishnan R, Kanniappan GV, Pandurangan V, Jayaraman S, Dhayalan VK, Mironescu M, Mironescu ID, Palanisamy CP. Antioxidant and biocompatible CuO-starch/PVA nanoscaffolds via ultrasonic green synthesis using Turbinaria conoides (brown marine macroalgae). Medicine in Drug Discovery. 2025; 28: 100238.
[15] Gong J, Lin J, Guan T, Pei J, Palanisamy CP, El-AtyFrom AMA. selenium tolerance to nanoplastic antagonism: Comprehensive characterization of L. casei SNUT1 and its extracellular vesicle–nanoselenium complex. Food Bioscience. 2025; 74: 107749.
[16] Poochi SP, Sundarraj R, Raju MV, Chandrasekaran MK, Ahalliya RM, Palanisamy CP, Kanniappan GV, Kondapavuluri BK, Thiruvengadam M. Harnessing Nature: Computational and Experimental Insights Into *Ipomoea obscura* Metabolites for Bladder Cancer Therapy. Chemistry and Biodiversity. 2025; 0: e00909.
[17] Dugganaboyana GK, Kannankumar MKG, Shivaramakrishna S, Raju MV, Chandrasekaran MK, Ahalliya RM, Panneerselvam N, Palanisamy CP, Kanniappan GV. Phytochemical insights, antioxidant activity and therapeutic potential of Cassia senna against prostate cancer in Wistar albino rats. Discover Applied Sciences. 2025; 7:1206.
[18] Natarajan SR, Krishnamoorthy R, Alshuniaber MA, Gatasheh MK, Rajagopal P, Veeraraghavan VP, Palanisamy CP, Jayaraman S. KDM1A Facilitates Oncogenic Potential in Colorectal Cancer Progression Through the Activation of AXIN/GSK3β/β-Catenin Signaling Pathways: Evidence From Integrated Transcriptomics and In Vitro Studies. The Journal of Gene Medicine. 2025; 27(11): e70053.
[19] Guan T, Gong J, Lin J, Palanisamy CP, Jinjin Pei J, El-Aty AMA. Machine learning-driven multimodal optimization of selenium biotransformation and flavor profiling in fermented apple–Yacon functional beverages. Innovative Food Science & Emerging Technologies. 2025; 105: 104198.
[20] Natarajan SR, Krishnamoorthy R, Alshuniaber MA, Alsulami TS, Gatasheh MK, Rajagopal P, Palanisamy CP, Govindan R, Veeraraghavan VP, Jayaraman S. ABCE1 facilitates tumour progression via aerobic glycolysis and inhibits cell death in human colorectal cancer cells through the p53 signalling pathway. Scientific Reports. 2025; 15: 24674.
[21] Huang Y, Guo H, Liu Y, Jin W, Palanisamy CP, Pei J, Oz F, El-Aty AMA. Effects of Natural Polysaccharides on the Gut Microbiota Related to Human Metabolic Health. Molecular Nutrition & Food Research. 2025; 69:e202400792.
[22] Poornima K, Meenakshi K.C, Manikandan V.R, Shankari G, Prabhu D, Rathi M.A, Palanisamy CP, Balaji R, Gopalakrishnan V.K. Exploring the anticancer potential of Jerantinine A from *Tabernaemontana coronaria* against prostate, breast, and ovarian cancers: A computational approach. *Journal of Complementary and Integrative Medicine*, 2025 22(2): 363–372.
[23] Palanisamy CP, Poompradub S, Sansanaphongpricha K, Jayaraman S, Subramani K. Faridah Sonsudin gGreen synthesis of Nigella sativa-mediated silver nanoparticles for enhanced antibacterial activity and wound healing: Mechanistic insights and biomedical applications. Environmental Nanotechnology, Monitoring & Management. 2025; 24: 101085.

[24] Surendran N, Raju MV, Chandrasekaran MK, Ahalliya RM, Palanisamy CP, Chandrasekaran G, Kanniappan GV. Physicochemical characterization of starch from Maranta arundinacea L.(arrowroot) rhizomes and its inhibition of COX-2: In vivo validation. Bioactive Carbohydrates and Dietary Fibre. 2025; 33: 100465.
[25] Kannappan P, Chandrasekaran MK, Raju MV, Gopalakrishnan S, Dhamodharan P, Ahalliya RM, Palanisamy CP, Raju B, Kanniappan GV. Exploring the anticancer potential of Jerantinine A from Tabernaemontana coronaria against prostate, breast, and ovarian cancers: a computational approach. Journal of Complementary and Integrative Medicine. 2025; 22(02): 363-372.
[26] Pei J, Kumarasamy RV, Jayaraman S, Kanniappan GV, Long Q, Palanisamy CP. Quercetin-functionalized nanomaterials: Innovative therapeutic avenues for Alzheimer's disease management. Ageing Research Reviews. 2025; 104: 102665.
[27] Natarajan PM, Swamikannu B, Sivaraman NM, Stylin AGSQ. Prevention of Oral Cancer: A Comprehensive Guide. Journal of Pharmacy and Bioallied Sciences. 2024; 16(5): S4239-S4241.
[28] Umapathy V, Dhanavel A, Kesavan R, Natarajan PM, Bhuminathan S, Vijayalakshmi P. Anticancer Potential of the Principal Constituent of Piper nigrum, Piperine: A Comprehensive Review. Cureus. 2024; 16(2): e54425.
[29] Umapathy VR, Swamikannu B, Natarajan PM, Devi R, Nandini MS, Vimalarani, Vijayalakshmi P. In Silico Molecular Docking of Ocimum sanctum Phytochemicals: Targeting Key Biomarkers in Oral Cancer. Journal of Pharmacy and Bioallied Sciences. 2024; 16(5): S4792-S4799.
[30] Natarajan PM, Bhuminathan S, Rajan R, Bindu K, Loganathan K, Veerakumar R. The Crucial Role of Smoking Cessation in Preventing Oral Cancer. Journal of Pharmacy and Bioallied Sciences. 2024; 16(5): S4245-S4247.
[31] Swamikannu B, Umapathy VR, Natarajan PM, Nandini MS, Stylin AGSQ, Vimalarani V, Rajinikanth S. Unlocking the Therapeutic Benefits of Artemisia Annua: A Comprehensive Overview of its Medicinal Properties. Journal of Pharmacy and Bioallied Sciences. 2024; 16(5): S4248-S4253.
[32] Natarajan PM. Computational Studies on Recent Congeners of Fluoroquinolones and Nitroimidazoles for Their Use in Periodontal Therapy. Journal of Pharmacy and Bioallied Sciences. 2024; 16(5): S4731-S4740.
[33] Yadalam PK, Arumuganainar D, Natarajan PM, Ardila CM. Artificial intelligence-powered prediction of AIM-2 inflammasome sequences using transformers and graph attention networks in periodontal inflammation. Scientific Reports. 2025; 15: 8733.
[34] Yadalam PK, Chatterjee S, Natarajan PM, Ardila CM. Comparison of light gradient boosting and logistic r egression for interactomic hub genes in Porphyromonas gingivalis and Fusobacterium nucleatum-induced perio dontitis with Alzheimer's disease. Frontiers in Oral Health. 2025; 6:1463458.
[35] Natarajan PM, Bhuminathan S, Leela B, Bindu K, Loganathan K, Ramachandran V. Smoking and its Role in Oral Cancer. Journal of Pharmacy and Bioallied Sciences 16(5): S4242-S4244.
[36] Yadalam PK, Natarajan PM, Ardila CM. Variational graph autoencoder for reconstructed transcriptomic data associated with NLRP3 mediated pyroptosis in periodontitis. Scientific Reports. 2025; 15: 1962.
[37] Jayaraman S, Prasad M, Natarajan SR, Krishnamoorthy R, Alshuniaber MA, Gatasheh MK, Veeraraghavan VP, Rajagopal P, Palanisamy CP. Molecular mechanisms underlying the effects of beta-sitosterol on TGF-β1/Nrf2/SIRT1/p53-mediated signaling in the kidney of a high-fat diet and sucrose-induced type-2 diabetic rat. Chemico-Biological Interactions. 2025; 411: 111443.
[38] Huang Y, Guo H, Liu Y, Jin W, Palanisamy CP, Pei J, Oz F, El-Aty AMA. Effects of Natural Polysaccharides on the Gut Microbiota Related to Human Metabolic Health. Molecular Nutrition & Food Research. 2025; e202400792.
[39] Prabhakaran P, Palanisamy CP, Shanmugam A, Damodharan P, Swaminathan H, Devaraj D, Ahalliya RM, Kanniappan GV. Isolation, structural characterization, and molecular docking studies on the bioactive compound from n-Hexane extract of Emilia sonchifolia (L.) DC against the pancreatic cancer target Aurora 2 Kinase. Journal of Complementary and Integrative Medicine. 2024; 22(1): 0290.
[40] Jiang H, Kumarasamy RV, Pei J, Raju K, Kanniappan GV, Palanisamy CP. Integrating engineered nanomaterials with extracellular vesicles: Advancing targeted drug delivery and biomedical applications. Frontiers in Nanotechnology. 2024; 6: 1513683.
[41] Guo H, Liu Y, Wan T, Song D, Palanisamy CP, Geng J, Pei J, Özmen S, El-Aty AMA. Toward personalized cancer management: Role of precision nutrition–diet interventions. Journal of Functional Foods. 2024; 123: 106584.
[42] Natarajan SR, Krishnamoorthy R, Alshuniaber MA, Al-Anazi KM, Farah MA, Rajagopal P, Palanisamy CP, Veeraraghavan VP, Jayaraman S. Identification of FOXM1 as a novel protein biomarker and therapeutic target for colorectal cancer progression: Evidence from immune infiltration and bioinformatic analyses. International Journal of Biological Macromolecules. 282 (Part 4): 137201.
[43] Rajendran MS, Jayaraman S, Khan JM, Jasmine S, Prabhakaran RK, Raju MV, Chandrasekaran MK, Ahalliya RM, Kannappan P, Palanisamy CP, Kanniappan GV. Investigating the colon toxicity and carcinogenic role of monosodium glutamate compared with Dimethylhydrazine in male Wistar rats: Exploring the link to childhood colon cancer risk. Journal of King Saud University - Science. 2024; 36(11): 103507.
[44] Kumarasamy RV, Natarajan P, Umapathy VR, Roy JR, Rab SO, Saeed M, Panagal M, Mironescu M, Srinivasan GP, Palanisamy CP. Clinical Applications and Therapeutic Potentials of Advanced Nanoparticles: A Comprehensive Review on Completed Human Clinical Trials. Frontiers in Nanotechnology. 2024; 6:1479993.

[45] Jin W, Pei JJ, Roy JR, Jayaraman S, Ahalliya RM, Kanniappan GV, Mironescu M, Palanisamy CP. Comprehensive review on single-cell RNA sequencing: A new frontier in Alzheimer's disease research. Ageing Research Reviews. 2024; 274: 102454.
[46] Pei J, Palanisamy CP, Jayaraman S, Natarajan PM, Umapathy VR, Roy JR, Panagal M, Jayaraman S. Curcumin-loaded polymeric nanomaterials as a novel therapeutic strategy for Alzheimer's disease: A comprehensive review. Ageing Research Reviews. 2024; 99: 102393.
[47] Pei J, Palanisamy CP, Jayaraman S, Natarajan PM, Umapathy VR, Roy JR, Thalamati D, Ahalliya RM, Kanniappan GV, Mironescu M. A comprehensive review on starch-based Sustainable Edible Films Loaded with Bioactive Components for Food Packaging. International Journal of Biological macromolecules. 2024; 274 (Part-1): 133332.
[48] Palanisamy CP, poompradub S, Sansanaphongpricha K, Subramani K, Sonsudin F. Increased expression levels of PDGF and VEGF magnify the wound healing potential facilitated by biogenic synthesis of silver nanoparticles. Nano-Structures & Nano-Objects. 2024; 39: 101236.
[49] Pei J, Palanisamy CP, Jayaraman S, Natarajan PM, Umapathy VR, Roy JR, Thalamati D, Ahalliya RM, Kanniappan GV, Mironescu M. Proteomics Profiling of Extracellular Vesicle for Identification of Potential Biomarkers in Alzheimer's Disease: A Comprehensive Review. Ageing Research Reviews. 2024; 99: 102359.
[50] Xi J, Wang T, Xian P, Liu X, Du M, Yang H, Palanisamy CP, Lin W, Long Q. Proteomic insights uncover enhanced neurotherapeutic potential in conditioned mesenchymal stem cell-derived extracellular vesicles. Extracellular Vesicle. 2024; 3: 100037.
[51] Pei J, Natarajan PM, Umapathy VR, Swamikannu B, Sivaraman NM, Krishnasamy L, Palanisamy CP. Advancements in the synthesis and functionalization of zinc oxide-based nanomaterials for enhanced oral cancer therapy. Molecules. 2024; 29(11): 2706.
[52] Gatasheh MK, Natarajan SR, Krishnamoorthy R, Alsulami TS, Rajagopal P, Palanisamy CP, Veeraraghavan VP, Jayaraman S. Molecular analysis to identify novel potential biomarkers as drug targets in colorectal cancer therapy: an integrated bioinformatics analysis. Molecular and Cellular Oncology. 2024; 11(1): 2326699.
[53] Pei J, Yan Y, Jayaraman S, Rajagopal P, Natarajan PM, Umapathy VR, Gopathy S, Roy JR, Sadagopan CS, Thalamati D, Palanisamy CP, Mironescu M. A review on advancements in the application of starch-based nanomaterials in biomedicine: Precision drug delivery and cancer therapy. International Journal of Biological Macromolecules. 2024; 130746.
[54] Pei JJ, Yan Y, Palanisamy CP, Jayaraman S, Natarajan PM, Umapathy VR, Gopathy S, Roy JR, Sadagopan JC, Thalamati D, Mironescu M. Materials-based drug delivery approaches: Recent advances and future perspectives. Green Processing and Synthesis. 2024; 13: 20230094.
[55] Pei JJ, Deng W, Liu Y, Guo Y, Chen J, Abdu H, Khan MR, Palanisamy CP, El-Aty AM. A Comprehensive Review of Cornus officinalis: Health Benefits, Phytochemistry, and Pharmacological Effects for Functional Drug and Food Development. Frontiers in Nutrition. 2023; 10: 1309963.
[56] Alugoju P, Palanisamy CP, Anthikapalli NVA, Jayaraman S, Prasanskulab A, Chuchawankul S, Dyavaiah M, Tencomnao T. Exploring the anti-aging potential of natural products and plant extracts in budding yeast Saccharomyces cerevisiae: A review. F1000Research. 2023; 12: 1265.
[57] Lavanya M, Krishnamoorthy R, Alshuniaber MA, Manoharadas S, Palanisamy CP, Veeraraghavan VP, Jayaraman S, Rajagopal P, Padmini R. Formulation, characterization and evaluation of gelatin-syringic acid/zinc oxide nanocomposite for its effective anticancer, antioxidant and anti-inflammatory activities. Journal of King Saud University-Science. 2023; 35: 102909.
[58] Palanisamy CP, Poompradub S, Sansanaphongpricha K, Jayaraman S, Subramani K, Sonsudin F. Biosynthesis of silver nanoparticles (AgNPs) using ethanolic extract of Nigella sativa (L.) seeds promotes wound healing via PDGF and VEGF signalling pathways activation. Biocatalysis and Agricultural Biotechnology. 2023; 54: 102970.
[59] Prasad M, Jayaraman S, Natarajan SR, Veeraraghavan VP, Krishnamoorthy R, Gatasheh MK, Palanisamy CP, Elrobh M. Piperine modulates IR/Akt/GLUT4 pathways to mitigate insulin resistance: Evidence from animal and computational studies. International Journal of Biological Macromolecules. 2023; 253: 127242.
[60] Palanisamy CP, Pei JJ, Phaniendra A, Venkata AAN, Jayaraman S, Veeraragahavan VP, Sridevi G, Roy JR, Janaki CS, Thalamati D, Mironescu M, Luo Q, Chai Y, Long Q. New Strategy of Neurodegenerative Disease Treatment with Extracellular Vesicles (EVs) Derived from Mesenchymal Stem Cells (MSCs). *Theranostics*. 2023; 13(12):4138-4165. doi:10.7150/thno.83066.
[61] Palanisamy CP, Phaniendra A, Jayaraman S, Poompradub S. *Nigella sativa* L. seed extracts promotes wound healing progress by activating VEGF and PDGF signalling pathways: *An in vitro* and *in silico* study. *F1000 Research*. 2023; 12: 436.
[62] Pei JJ, Palanisamy CP, Phaniendra A, Venkata AAN, Natarajan PM, Umapathy VR, Swamikannu B, Jayaraman S, Rajagopal P, Poompradub S. A comprehensive review on bio-based materials for chronic diabetic wounds. *Molecules*. 2022; 28(2), 604.
[63] Palanisamy CP, Cui B, Zhang H, Gunasekaran VP, Ariyo A, Jayaraman S, Veeraraghavan V, Rajagopal P. A critical review on starch-based electrospun nanofibrous scaffolds for wound healing application. International Journal of Biological Macromolecules. 2022; 222 (Part: B): 1852-1860.

[64] Monisha P, Ponnulakshmi R, Nalini D, Vishnu P V, Palanisamy CP, Cui B, Shankargouda P, Selvaraj J. A comprehensive review on high fat diet-induced diabetes mellitus: An epigenetic view. The Journal of Nutritional Biochemistry. 2022; 2022: 109037.
[65] Monisha P, Selvaraj J, Mohamed AE, Mohamed E, Mosaab AEA, Vishnu PV, Srinivasan V, Vidhya RU, Shazia FJH, Kalaiselvi K, Durairaj S, Palanisamy CP, Surapaneni K M, Ponnulakshmi R. A Comprehensive review on therapeutic perspectives of phytosterols in insulin resistance: A mechanistic approach. Molecules. 2022; 27(5): 1595.
[66] Natarajan PM, Umapathy VR, Murali A, Swamikannu B. (2022). Computational Simulations of Identified marine-derived Natural Bioactive Compounds As Potential Inhibitors of Oral Cancer. Future Science OA. 2022; 8(3).
[67] Natarajan PM, Umapathy VR. Role of transcriptomics in the study of oral cancer. Frontiers in Oral Health. 2025; 6:1524364.
[68] Vidhyarekha U, Natarajan PM, Bhuminathan S, Sabarinathan J, Suba R, Vijayalakshmi P. Role of artificial intelligence in Oral Cancer. Advances in Public Health. 2024. 2024: 3664408.
[69] Ganesan A, Kumar NG, Natarajan PM, Gauthaman J. Automated classification of elongated styloid processes using deep learning models-an artificial intelligence diagnostics. Frontiers in Oral Health. 2025; 5: 1424840.
[70] Umapathy VR, Natarajan PM, Swamikannu B. Regenerative Strategies in Dentistry: Harnessing Stem Cells, Biomaterials and Bioactive Materials for Tissue Repair. Biomolecules. 2025; 15: 546.
[71] Natarajan PM. Dental Bioinformnatics-Current Scope and Future perspectives. Research Journal of Pharmacy and Technology. 2022;15(5):2351-6.
[72] Ganesan A, Kumar NG, Natarajan PM. Solanum trilobatum leaf extract-derived silver nanoparticles downregulate the PI3K/AKT/mTOR signaling pathway and attenuate oral squamous cell carcinoma cell proliferation. Journal of Herbmed Pharmacology. 2024; 13(2): 300-307.
[73] Perumal MKK, Renuka RR, Subbiah SK, Natarajan PM. Artificial intelligence-driven clinical decision support systems for early detection and precision therapy in oral cancer: a mini review. Frontiers in Oral Health. 2025; 6: 1592428.
[74] Ramesh E, Ganesan A, Lakshmi KC, Natarajan PM. Artificial intelligence-based diagnosis of oral leukoplakia using deep convolutional neural networks Xception and MobileNet-v2. Frontiers in Oral Health. 2025; 6: 1414524.
[75] Ganesan A, Kumar NG, Natarajan PM. Anticancer activity of silver nanoparticles synthesized from aqueous leaf extract of Solanum trilobatum (Purple fruit pea eggplant) on human oral cancer cells. Journal of Herbmed Pharmacololgy. 2024; 13(2): 260-268.
[76] Pei JJ, Perumal NC, Meng P, Long Q, Palanisamy CP. AI-assisted FTIR spectroscopic profiling of exosomes: Emerging frontiers in early detection of Alzheimer's disease. Ageing Research Reviews. 2026; 103311.
[77] Raja FSD, Abraham L, Rangasamy K, Saikia K, Rathankumar AK, Mironescu M, Mironescu I, Palanisamy CP, Kanniappan GV. Next-Generation Microbiome Therapeutics: Psychobiotics and Fecal Microbiota Transplants (FMT) for Mental Health Treatment. Frontiers in Cellular and Infection Microbiology. 2026; 16: 1719357.
[78] Subramani K, Srinivasan S, Shanmugam P, Palanisamy CP, Sonsudin F, Poompradub S. Sustainable phytochemical mediated-ZnO nanoparticles derived from Crescentia cujete for toxicological evaluation and multifunctional environmental applications. Environmental Nanotechnology, Monitoring & Management. 2026; 26: 101180.
[79] Kunamalla RP, Panagal M, Palanisamy CP. Green-engineered multiscale starch/PVA nanofibrous scaffolds embedded with CuO nanoparticles from Sargassum ilicifolium for potent antimicrobial performance. Genetics and Molecular Research. 2026; 25(13s): 1-9.
[80] Dharmaprakash S, Gunasekaran VP, Sivaramakrishnan R, Kanniappan GV, Jayaraman S, Mironescu M, Rajabathar JR, Mironescu ID, Palanisamy CP. Marine macroalgae-mediated ultrasonic-assisted green synthesis of CuO nanoparticles embedded in starch/PVA electrospun nanoscaffolds for in vitro α-amylase and α-glucosidase inhibitory activity. Scientific Reports. 2026; 16: 26243.